Available online at www.sciencedirect.com
SCIENCE DIRECT®
Electrochimica Acta 51 (2005) 731–738
ELECTROCHIMICA Acta
www.elsevier.com/locate/electacta

Analysis of the use of voltammetric results as a steady state approximation to evaluate kinetic parameters of the hydrogen evolution reaction

C.A. Marozzi [a], M.R. Canto [b], V. Costanza [b], A.C. Chialvo [a,*,1]

[a] *Programa de Electroquímica Aplicada e Ingeniería Electroquímica (PRELINE), Facultad de Ingeniería Química, Universidad Nacional del Litoral, Santiago del Estero 2829, 3000 Santa Fe, Argentina*
[b] *Instituto de Desarrollo Tecnológico para la Industria Química (INTEC), Universidad Nacional del Litoral-Consejo Nacional de Investigaciones Científicas y Técnicas, Güemes 3450, 3000 Santa Fe, Argentina*

Received 14 January 2005; received in revised form 1 April 2005; accepted 29 May 2005
Available online 7 July 2005

Abstract

The use of the voltammetric response $j^{vol}(\eta)$ of a potentiodynamic sweep at a slow scan rate v_s in place of a steady state polarization curve $j^{ss}(\eta)$ for the determination of the kinetic parameters of the hydrogen evolution reaction is analyzed. It is proposed to consider $j^{vol}(\eta, v_s) \cong j^{ss}(\eta)$ when the condition $0.99 \leq j^{vol}(\eta, v_s)/j^{ss}(\eta) \leq 1.01$ is verified in the overpotentials range $\eta \leq -0.05$ V. It has been also established a simple relationship between the maximum admissible scan rate v_s^{max} and the equilibrium polarization resistance R_p. Finally, the application of this criterion on different electrodes is described and discussed.

Keywords: Hydrogen evolution reaction; Kinetic parameters; Steady state approximation

1. Introduction

The determination of the elementary kinetic parameters of the hydrogen evolution reaction (her) is often carried out from the experimental dependence of the current density j^{exp} on the overpotential η, resulting from the application of a potentiodynamic sweep run at slow scan rates v_s [1–8]. The values of the experimental voltammetric current density $j^{exp}(\eta, v_s)$ are then substituted in theoretical steady state expressions of a given kinetic mechanism in order to obtain the corresponding values of the kinetic parameters. In this context, it should be of interest to study the conditions in which $j^{exp}(\eta, v_s)$ can be considered sufficiently approximated to the corresponding steady state current density $j^{ss}(\eta)$.

From a theoretical point of view, the voltammetric current density $j^{vol}(\eta, v_s)$ can be described as a sum of two contributions, one corresponding to the electrode reaction $j^r(\eta, v_s)$ and the other originated in the double layer capacitance $j^c(\eta, v_s)$ [9],

$$j^{vol}(\eta, v_s) = j^r(\eta, v_s) + j^c(\eta, v_s) \quad (1)$$

where $j^r(\eta, v_s)$ involves the Faradaic (charge required for the whole electrode reaction) and the transient pseudocapacitive (charge required to change the surface coverage) contributions. Besides, the effect of the adsorption of the reaction intermediate on the double layer charge in $j^c(\eta, v_s)$ was considered negligible [9]. These two components of the voltammetric current density are characterized by fulfilling the following limits:

$$\lim_{v_s \to 0} j^r(\eta, v_s) = j^{ss}(\eta) \quad (2)$$

* Corresponding author. Tel.: +54 342 4571164; fax: +54 342 4571162.
E-mail address: achialvo@fiqus.unl.edu.ar (A.C. Chialvo).
[1] ISE member.

0013-4686/$ – see front matter © 2005 Elsevier Ltd. All rights reserved.
doi:10.1016/j.electacta.2005.05.040

$$\lim_{v_s \to 0} j^c(\eta, v_s) = 0 \tag{3}$$

and therefore,

$$\lim_{v_s \to 0} j^{vol}(\eta, v_s) = j^{ss}(\eta) \tag{4}$$

The limiting behavior given in Eq. (4) is a justification for the use of slow potentiodynamic sweeps as an approximation to the steady state. Nevertheless, a quantitative basis for the adoption of a given sweep rate could be useful. Then, the maximum scan rate v_s^{max}, from which the following approximation:

$$j^{vol}(\eta, v_s \leq v_s^{max}) \cong j^{ss}(\eta) \tag{5}$$

can be considered valid, needs to be determined.

In this context, the present work evaluates theoretically the variation of the current densities $j^{vol}(\eta, v_s)$ and $j^{ss}(\eta)$ for the hydrogen evolution reaction under the Volmer–Heyrovsky–Tafel mechanism on a wide range of the kinetic parameters values. Starting from the analysis of such dependences, a criterion for the selection of the maximum admissible sweep rate v_s^{max} is proposed on the basis of the equilibrium polarization resistance.

2. Theoretical analysis

In order to find the conditions in which Eq. (5) is accomplished, a theoretical expression for the current density dependence given in Eq. (1) must be derived. The Faradaic and transient pseudocapacitive contributions involved in $j^r(\eta, v_s)$ will be evaluated from the Volmer–Heyrovsky–Tafel mechanism,

$$H_2O + e^- + S \rightleftarrows H_{(ad)} + OH^- \quad \text{Volmer} \tag{6a}$$

$$H_{(ad)} + H_2O + e^- \rightleftarrows H_{2(g)} + OH^- + S \quad \text{Heyrovsky} \tag{6b}$$

$$H_{(ad)} + H_{(ad)} \rightleftarrows H_{2(g)} + 2S \quad \text{Tafel} \tag{6c}$$

where S is the active site for the adsorption of the reaction intermediate $H_{(ad)}$, usually named as overpotential deposited hydrogen (H_{OPD}) [9,10]. The reaction rates of these elementary steps are described, on the basis of a Langmuir-type adsorption (this assumption will be justified in Section 3), by the following expressions [1],

$$\frac{v_V(\eta, v_s)}{v_V^e} = \left[\frac{1-\theta}{1-\theta^e} e^{-(1-\alpha)f\eta} - \frac{\theta}{\theta^e} e^{\alpha f\eta}\right] \tag{7a}$$

$$\frac{v_H(\eta, v_s)}{v_V^e} = m_H \left[\frac{\theta}{\theta^e} e^{-(1-\alpha)f\eta} - \frac{1-\theta}{1-\theta^e} e^{\alpha f\eta}\right] \tag{7b}$$

$$\frac{v_T(\eta, v_s)}{v_V^e} = m_T \left[\left(\frac{\theta}{\theta^e}\right)^2 - \left(\frac{1-\theta}{1-\theta^e}\right)^2\right] \tag{7c}$$

where v_i is the rate of the step i (i = V, H, T), θ the surface coverage of the adsorbed hydrogen $H_{(ad)}$, α is the symmetry factor (considered the same for the Volmer and Heyrovsky steps), $f = F/RT$ and $m_i = v_i^e/v_V^e$ ($i = H, T$). The superscript 'e' indicates equilibrium conditions and it has been taken negative values for η in the cathodic direction.

Expressions (7a)–(7c) involve the dependence of the surface coverage on the overpotential and on the sweep rate, $\theta = \theta(\eta, v_s)$. This relationship can be determined from the following mass balance for the adsorbed hydrogen $H_{(ad)}$ [9],

$$\frac{dn_{H_{(ad)}}}{dt} = v_V - v_H - 2v_T \tag{8}$$

where $n_{H_{(ad)}}$ is the number of moles of $H_{(ad)}$ per unit of electrode area. It should be noticed that when $dn_{H_{(ad)}}/dt = 0$, the steady state is achieved and the reaction contribution is purely Faradaic. Taking into account that the scan rate of the potentiodynamic sweep is $v_s = d\eta/dt$, Eq. (8) can be written as [9],

$$\frac{d\theta(\eta, v_s)}{d\eta} = F\frac{(v_V - v_H - 2v_T)}{v_s\sigma} = \frac{F}{v_V^e}\left(\frac{v_V - v_H - 2v_T}{m_s\sigma}\right) = \frac{C_\theta^t(\eta, v_s)}{\sigma} \tag{9}$$

where the parameter m_s was defined as $m_s = v_s/v_V^e$, σ is the electric charge corresponding to a $H_{(ad)}$ monolayer, which was considered equal to 220 μC cm^{-2}, F the Faraday constant and $C_\theta^t(\eta, v_s)$ is the transient adsorption pseudocapacitance.

In this context, the reaction current density $j^r(\eta, v_s)$ is related to the rates of the elementary steps by [9],

$$j^r(\eta, v_s) = F(v_V + v_H) \tag{10}$$

Furthermore, the capacitance contribution $j^c(\eta, v_s)$ can be evaluated from the following equation:

$$j^c(\eta, v_s) = cv_s = cv_V^e m_s \tag{11}$$

where c represents the double layer capacitance, which will be considered constant on the range of potentials used in this study.

The dependences $j^{vol}(\eta, v_s)$ and $\theta(\eta, v_s)$ resulting from the application of a potentiodynamic sweep can be obtained from the resolution of the system of Eqs. (1), (7a)–(7c) and (9)–(11) for a given set of the kinetic parameters. Furthermore, the steady state current density $j^{ss}(\eta)$ can be determined from the same system of equations, with the following additional condition $dn_{H_{(ad)}}/dt = 0$.

3. Results and discussion

The system of Eqs. (1), (7a)–(7c) and (9)–(11) was numerically solved for the simultaneous occurrence of the Volmer, Heyrovsky and Tafel steps. The study was carried out on the overpotential range $-0.4\,V \leq \eta \leq 0\,V$, considering the electrode at equilibrium ($\eta = 0\,V$) as initial state. Simulations were performed at 30 °C, varying the parameter m_i (i = H, T) in the range $10^{-5} \leq m_i \leq 10^5$. The particular

cases corresponding to $m_T = 0$ (Volmer–Heyrovsky route) and $m_H = 0$ (Volmer–Tafel route) were also simulated. For the double layer capacitance a value of $c = 20\,\mu F\,cm^{-2}$ was adopted and α was fixed at 0.5. The equilibrium surface coverage was varied between the following values $10^{-5} \leq \theta^e \leq 10^{-1}$, since the experimental evidence shows that in general $\theta^e < 10^{-1}$ [2,11–14]. The parameter m_s was varied in the range $10^2 \leq m_s \leq 10^{12}$. Three potentiodynamic cycles were performed, within which a constant transient profile was always achieved. The calculated values of $j^{vol}(\eta, v_s)$ and $j^{ss}(\eta)$ were divided by the exchange current density of the Volmer step j_V^o, which is equal to Fv_V^e.

3.1. Analysis of the dependences $j^{vol}(\eta, v_s)$, $j^{ss}(\eta)$ and $\theta(\eta, v_s)$

More than two thousand simulations were needed in order to evaluate the dependences $j^{vol}(\eta, v_s)$, $j^{ss}(\eta)$ and $\theta(\eta, v_s)$ in the range of kinetic parameters values analyzed. Then, only a few cases were chosen in order to illustrate the results obtained.

Figs. 1 and 2 illustrate the case corresponding to the following values of the kinetic parameters: $\theta^e = 10^{-1}$, $m_H = m_T = 10^{-3}$ and $10^6 \leq m_s\ (V\,cm^2\,mol^{-1}) \leq 10^{10}$.

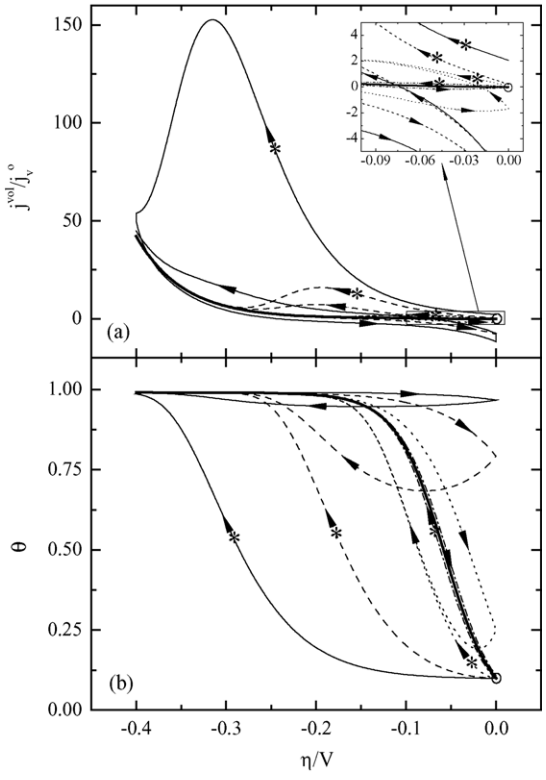

Fig. 1. Dependences (a) $j^{vol}(\eta, v_s)/j_V^o$ and (b) $\theta(\eta, v_s)$. $\theta^e = 10^{-1}$; $m_H = m_T = 10^{-3}$; $m_s\ (V\,cm^2\,mol^{-1})$: (– · · –) 10^6, (- · · · -) 10^7, (· · ·) 10^8, (- - -) 10^9, (—) 10^{10} and (▬) steady state; (◯) initial equilibrium state; (*) first hemicycle line. Arrows indicate the sense of the sweeps. Insert provides a magnification of the lower overpotentials region.

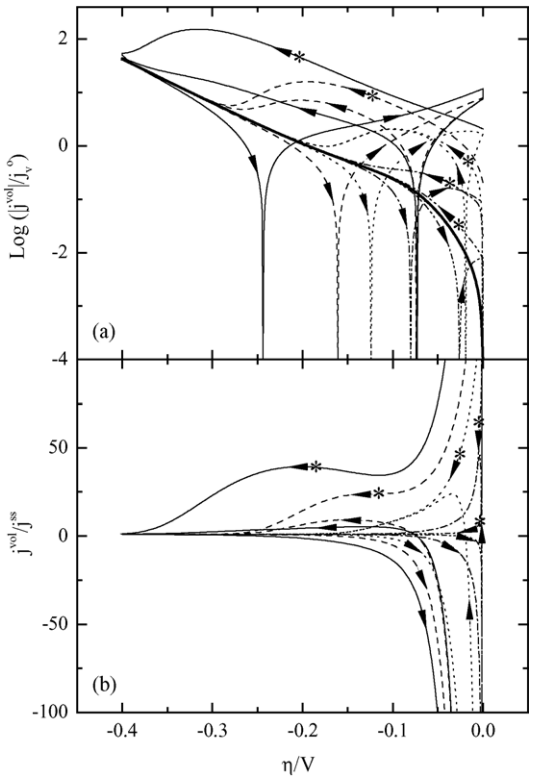

Fig. 2. Dependences (a) $\log[|j^{vol}(\eta, v_s)|/j_V^o]$ and (b) $j^{vol}(\eta, v_s)/j^{ss}(\eta)$. $\theta^e = 10^{-1}$; $m_H = m_T = 10^{-3}$; $m_s\ (V\,cm^2\,mol^{-1})$: (– · · –) 10^6, (- · · · -) 10^7, (· · ·) 10^8, (- - -) 10^9, (—) 10^{10} and (▬) steady state; (*) first hemicycle line. Arrows indicate the sense of the sweeps.

Fig. 1a shows the dependences $j^{vol}(\eta, v_s)/j_V^o$ (thin lines) at different m_s values and the corresponding dependence $j^{ss}(\eta)/j_V^o$ (thick line). It can be appreciated that for $m_s = 10^{10}\ V\,cm^2\,mol^{-1}$ (continuous thin line) the first hemicycle in the cathodic direction shows a well defined peak at ca. −0.32 V, which disappears in the following cycle. Then, as m_s decreases, the difference from the steady state response turns to be smaller, yet in the first voltammetric cycle. Another detail that should be noted is that $j^{vol}(\eta, v_s)/j_V^o$ changes its sign in both anodic and cathodic sweeps. This change takes place at potentials more cathodic than that corresponding to equilibrium and the difference becomes more important as m_s increases.

Fig. 1b shows the simulations of the dependence $\theta(\eta, v_s)$. The first cathodic hemicycle corresponding to $m_s = 10^{10}\ V\,cm^2\,mol^{-1}$ shows a strong increase of θ reaching a value near one, which is almost maintained in the following cycles. However, the decrease in m_s values produces a gradual approach of the potentiodynamic profile to that corresponding to the steady state, which is obtained for $m_s < 10^6\ V\,cm^2\,mol^{-1}$.

In order to emphasize the effect of the sweep rate (through m_s), data corresponding to Fig. 1a are depicted in different arrangements in Fig. 2. On this sense, Fig. 2a illustrates the logarithmic dependences of $|j^{vol}(\eta, v_s)|/j_V^o$ at different m_s values and of $j^{ss}(\eta)/j_V^o$ on overpotential. It can be more

clearly observed the inversion of the current sign because in this point $\log[|j^{vol}(\eta, v_s)|/j_V^o] \to -\infty$. This event is verified at potentials more cathodic than that corresponding to the equilibrium state as the value of m_s becomes higher.

Fig. 2b shows the relationship $j^{vol}(\eta, v_s)/j^{ss}(\eta)$, which clarifies the difference between the potentiodynamic response and that corresponding to the steady state. It can be appreciated that the deviation depends largely on potential, reaching the relationship the larger values at proximities of the equilibrium potential.

The results shown in Figs. 1 and 2 clearly indicates that, at least for the set of kinetic parameters used in this case, there is a critic m_s value ($\cong 10^4$) above which the condition given in Eq. (5) is not fulfilled.

Figs. 3 and 4 illustrate a case corresponding to the Volmer–Tafel route, with the following values of the kinetic parameters: $\theta^e = 10^{-3}$, $m_T = 10^{-5}$, $m_H = 0$ and $10^6 \le m_s$ (V cm^2 mol^{-1}) $\le 10^{10}$. The results shown in these figures are similar to those depicted in Figs. 1 and 2. It can be observed the presence in Fig. 3a ($m_s = 10^{10}$ V cm^2 mol^{-1}) of current peaks in both cathodic (ca. −0.32 V) and anodic (ca. −0.09 V) sweeps, respectively. Fig. 3a shows also the arising of a significant hysteresis process in the potentiodynamic simulations, which increases with the raise of m_s and leads to responses that are quite deviated from that of the steady state. This behavior is also observed in the dependence $\theta(\eta, v_s)$ (Fig. 3b). Points of inversion of the current sign are clearly visible in Fig. 4a as well as marked deviations from the steady state in the surroundings of the equilibrium potential (Fig. 4b). It should be noticed that Eq. (5) is fulfilled when $m_s \le 10^4$ V cm^2 mol^{-1}.

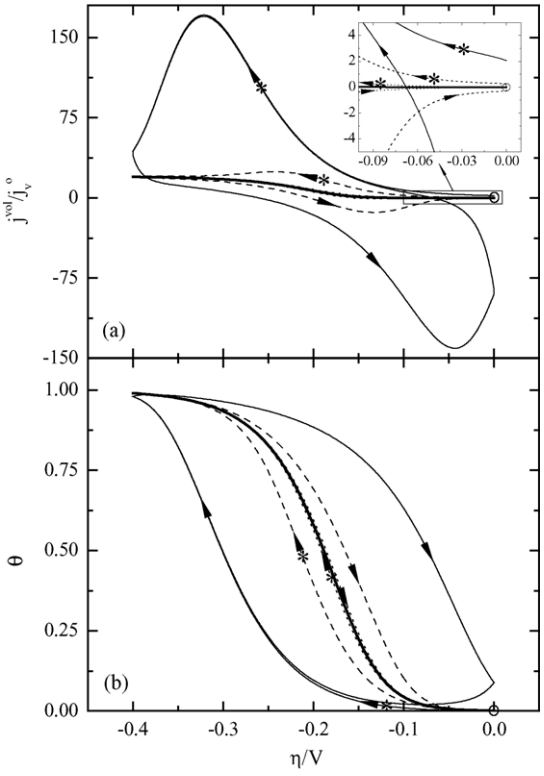

Fig. 3. Dependences (a) $j^{vol}(\eta, v_s)/j_V^o$ and (b) $\theta(\eta, v_s)$. $\theta^e = 10^{-3}$; $m_T = 10^{-5}$; $m_H = 0$; m_s (V cm^2 mol^{-1}): (–···–) 10^6, (-·-·-) 10^7, (···) 10^8, (- - -) 10^9, (—) 10^{10} and (▬) steady state; (◯) initial equilibrium state; (*) first hemicycle line. Arrows indicate the sense of the sweeps. Insert provides a magnification of the lower overpotentials region.

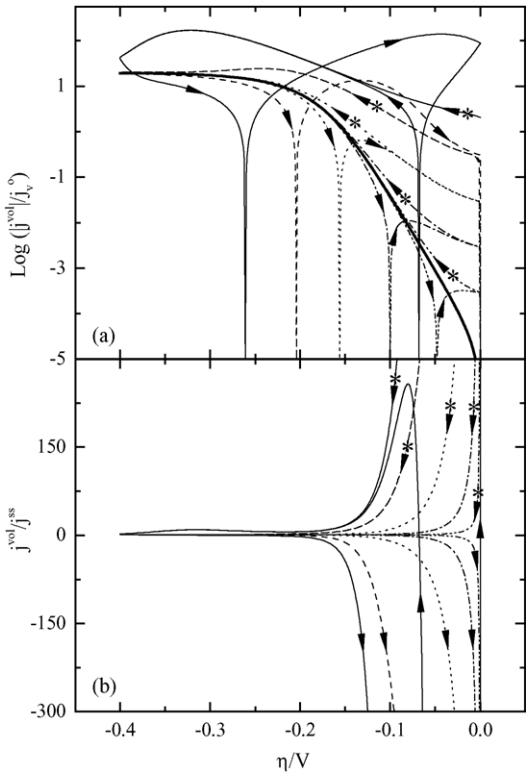

Fig. 4. Dependences (a) $\log[|j^{vol}(\eta, v_s)|/j_V^o]$ and (b) $j^{vol}(\eta, v_s)/j^{ss}(\eta)$. $\theta^e = 10^{-3}$; $m_T = 10^{-5}$; $m_H = 0$; m_s (V cm^2 mol^{-1}): (–···–) 10^6, (-·-·-) 10^7, (···) 10^8, (- - -) 10^9, (—) 10^{10} and (▬) steady state; (*) first hemicycle line. Arrows indicate the sense of the sweeps.

Finally, Figs. 5 and 6 show a case corresponding to the Volmer–Heyrovsky route, with the following values of the kinetic parameters: $\theta^e = 10^{-5}$, $m_H = 10^{-4}$, $m_T = 0$ and $10^8 \le m_s$ (V cm^2 mol^{-1}) $\le 10^{12}$. It can be observed again the fulfillment of Eq. (5) when $m_s \le 10^5$ V cm^2 mol^{-1}.

All the results shown above evidence that the use of potentiodynamic sweeps can produce dependences $j^{exp}(\eta, v_s)$ very different from the real ones, $j^{ss}(\eta)$. It can be also appreciated that the first hemicycle, which is usually employed in the experimental determinations, is the most inappropriate to obtain reliable results. Consequently, it is required to establish a criterion in order to determine aprioristically the conditions under which it is possible to accept reasonably that $j^{exp}(\eta, v_s) \cong j^{ss}(\eta)$.

3.2. Criterion for the selection of the sweep rate

As it has been already mentioned, it is necessary to find a criterion to select the rate of the potentiodynamic sweep, so that the experimental dependence $j^{exp}(\eta, v_s)$ obtained as

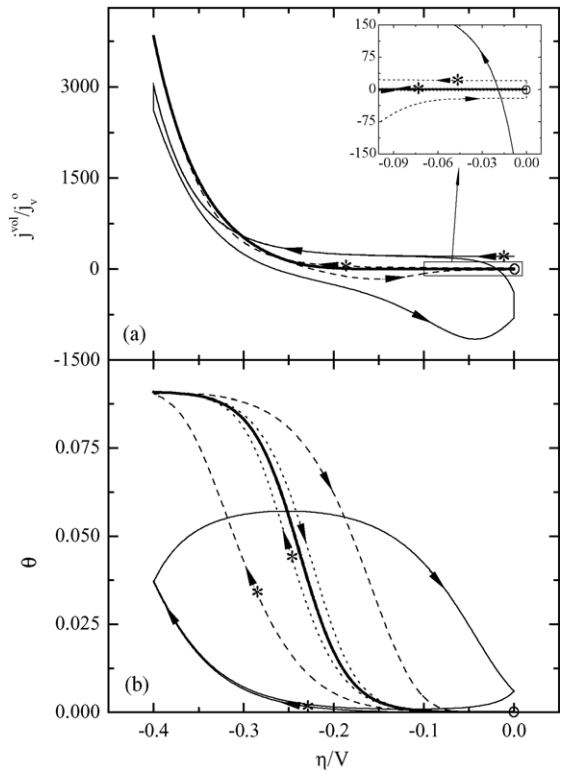

Fig. 5. Dependences (a) $j^{vol}(\eta, v_s)/j_V^o$ and (b) $\theta(\eta, v_s)$. $\theta^e = 10^{-5}$; $m_H = 10^{-4}$; $m_T = 0$; m_s (V cm^2 mol^{-1}): (–···–) 10^8, (-·-·-) 10^9, (···) 10^{10}, (- - -) 10^{11}, (—) 10^{12} and (▬) steady state; (◯) initial equilibrium state; (*) first hemicycle line. Arrows indicate the sense of the sweeps. Insert provides a magnification of the lower overpotentials region.

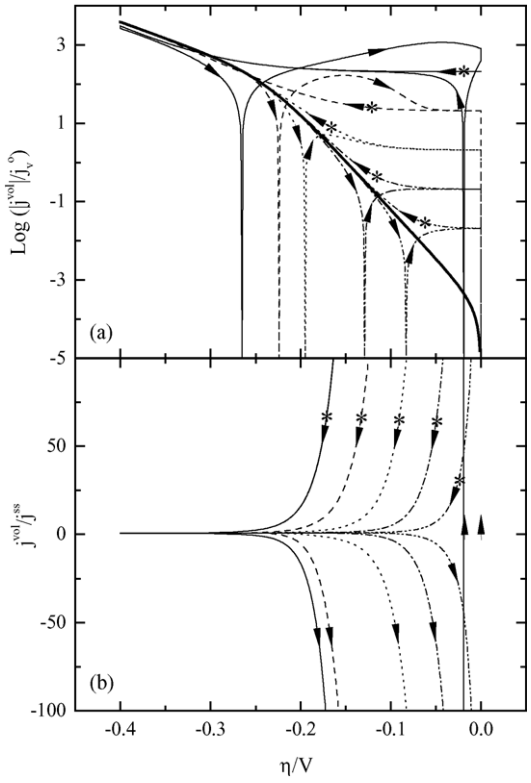

Fig. 6. Dependences (a) $\log[|j^{vol}(\eta, v_s)|/j_V^o]$ and (b) $j^{vol}(\eta, v_s)/j^{ss}(\eta)$. $\theta^e = 10^{-5}$; $m_H = 10^{-4}$; $m_T = 0$; m_s (V cm^2 mol^{-1}): (–···–) 10^8, (-·-·-) 10^9, (···) 10^{10}, (- - -) 10^{11}, (—) 10^{12} and (▬) steady state; (*) first hemicycle line. Arrows indicate the sense of the sweeps.

a transient response can be consider sufficiently close to that corresponding to the steady state.

The relationship between the voltammetric current density $j^{vol}(\eta, v_s)$ corresponding to the hemicycle where the potentiodynamic profile turns to be stabilized and that of the steady state $j^{ss}(\eta)$, was taken as a measure of the deviation from the steady state condition ($j^{vol}(\eta, v_s)/j^{ss}(\eta) = 1$). In this context, it is proposed to adopt as the maximum admissible sweep rate (v_s^{max}) that one that maintains this relationship inside a variation of ±1% from the unitary value,

$$0.99 \leq \frac{j^{vol}(\eta, v_s)}{j^{ss}(\eta)} \leq 1.01 \tag{12}$$

Furthermore, this condition must be fulfilled at least in the overpotentials range $\eta \leq -0.05$ V. Consequently, it is necessary to establish some measurable property that can be used as an indicator variable. It is proposed to utilize the equilibrium polarization resistance (R_p) of the her. This variable is related to the kinetic parameters according to the following expression [1],

$$R_p = \left.\frac{d\eta}{dj}\right]_{\eta=0} = \frac{RT}{4F^2 v_V^e} \frac{4m_T + m_H + 1}{m_H + m_T + m_H m_T} \tag{13}$$

Then, the relationship between this magnitude and the maximum admissible sweep rate was analyzed. At first, the following dependence of the maximum admissible value of the parameter m_s ($m_s^{max} = v_s^{max}/v_V^e$) was found through the numerical resolution of the system of Eqs. (1), (7a)–(7c) and (9)–(11) and the constrain given by Eq. (12):

$$m_s^{max} = f_1(m_H, m_T, \theta^e) \tag{14}$$

Then, the following theoretical functionality corresponding to the steady state (Eq. (13)), was determined,

$$R_p v_V^e = f_2(m_H, m_T) \tag{15}$$

Finally, a global dependence was established, on the basis of Eqs. (14) and (15),

$$R_p v_V^e m_s^{max} = R_p v_s^{max} = f_3(m_H, m_T, \theta^e) \tag{16}$$

The expression given in Eq. (16) was evaluated in the whole range of the parameters m_H, m_T and θ^e. This function is illustrated in Fig. 7 for the case of $\theta^e = 10^{-1}$. It was found that the minimum value obtained for this case is the lowest of the whole range of θ^e values. It can be appreciated that, all over the studied domain of the kinetic parameters values, the product $R_p v_s^{max}$ can be used as an aprioristic criterion to decide the validity of the approximation $j^{exp}(\eta, v_s) \cong j^{ss}(\eta)$. For instance, it can be observed from Fig. 7 that for $R_p v_s^{max} > 27[\log(R_p v_s^{max}) > 1.43]$, the condition given by Eq. (12) will never be fulfilled, independently of the values of the kinetic parameters m_H and m_T.

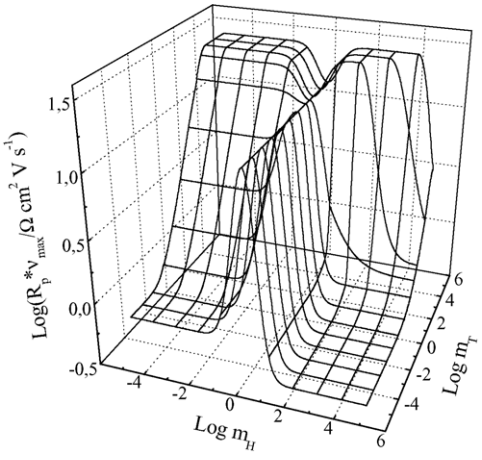

Fig. 7. Dependence of $\log(R_p v_s^{max})$ on $(\log m_H, \log m_T)$, fulfilling constrain given by Eq. (12). $\theta^e = 10^{-1}$.

On the other hand, when the following condition is accomplished $R_p v_s^{max} < 0.33[\log(R_p v_s^{max}) < -0.47]$, any system could fulfill the requirement established in Eq. (12).

It can be observed also that in the following domain, $0.33 < R_p v_s^{max} < 27[-0.47 < \log(R_p v_s^{max}) < 1.43]$, the validity of the condition imposed in Eq. (12) becomes uncertain. It should be noticed that in this case, if $m_H \cong 1$ and $10^{-5} \leq m_T \leq 10^5$ such condition is accomplished when $R_p v_s^{max} < 13.5[\log(R_p v_s^{max}) < 1.132]$. Meanwhile, if $m_T < 10^{-1}$ and $m_H < 10^{-1}$ the condition is fulfilled when $R_p v_s^{max} < 0.67[\log(R_p v_s^{max}) < -0.17]$.

From the results described above it can be inferred that, in order to fulfill the restriction imposed in Eq. (12), the absolute minimum of the function $f_3(m_H, m_T, \theta^e) = 0.33$ can be used as a reliable criterion for the selection of the sweep rate, and therefore,

$$v_s \leq \frac{0.33\,\Omega\,\mathrm{cm}^2\,\mathrm{V\,s}^{-1}}{R_p} \tag{17}$$

Any experimental dependence $j^{exp}(\eta, v_s)$ obtained from a potentiodynamic sweep with a scan rate lower or equal to that given by Eq. (17) will be able to be used for the evaluation of the elementary kinetic parameters corresponding to the steady state expressions of the hydrogen evolution reaction.

3.3. Selection of the adsorption model

It is well known that the behavior of the adsorbed reaction intermediate cannot be described by the Langmuir isotherm when the variation of the surface coverage on overpotential is considerable. Therefore, the use of a Frumkin-type adsorption should be more appropriate. In this case, Eqs. (7a)–(7c) should be replaced by [17],

$$\frac{v_V(\eta, v_s)}{v_V^e} = \left[\frac{1-\theta}{1-\theta^e} s^{-\lambda}\, e^{-(1-\alpha)f\eta} - \frac{\theta}{\theta^e} s^{(1-\lambda)}\, e^{\alpha f\eta}\right] \tag{18a}$$

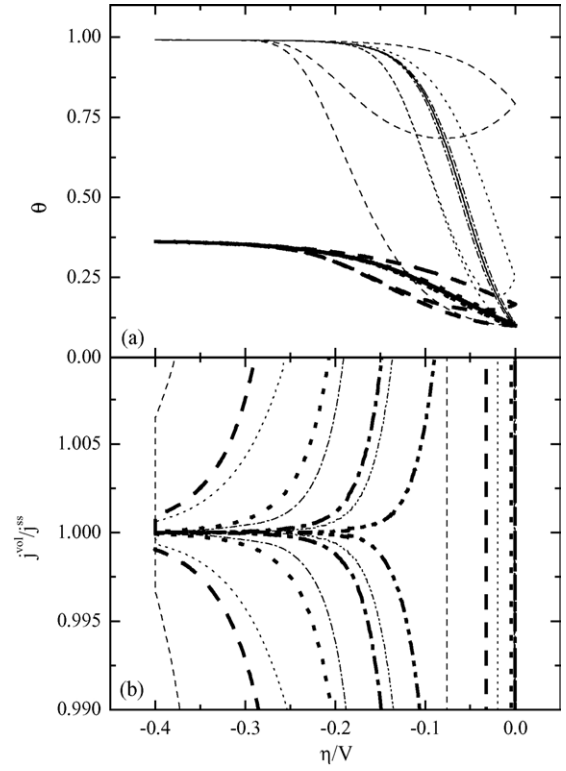

Fig. 8. Dependences (a) $\theta(\eta, v_s)$ and (b) $j^{vol}(\eta, v_s)/j^{ss}(\eta)$. $\theta^e = 10^{-1}$; $m_H = m_T = 10^{-3}$; m_s (V cm^2 mol^{-1}): (–···–) 10^6, (-·-·-) 10^7, (···) 10^8, (- - -) 10^9 and (—) steady state. First cycle not included in (b). Thin lines: Langmuir-type adsorption. Thick lines: Frumkin-type adsorption, $\lambda = 0.5$, $u = 20$.

$$\frac{v_H(\eta, v_s)}{v_V^e} = m_H \left[\frac{\theta}{\theta^e} s^{(1-\lambda)}\, e^{-(1-\alpha)f\eta} - \frac{1-\theta}{1-\theta^e} s^{-\lambda}\, e^{\alpha f\eta}\right] \tag{18b}$$

$$\frac{v_T(\eta, v_s)}{v_V^e} = m_T \left[\left(\frac{\theta}{\theta^e}\right)^2 s^{2(1-\lambda)} - \left(\frac{1-\theta}{1-\theta^e}\right)^2 s^{-2\lambda}\right] \tag{18c}$$

where $s = e^{u(\theta-\theta^e)}$, being u the interaction parameter in RT units and λ the adsorption symmetry factor. Fig. 8 shows the simulations (without the first cycle in Fig. 8b) obtained using Eqs. (18a)–(18c) in place of Eqs. (7a)–(7c). The parameters values are equal to those corresponding to Figs. 1 and 2 (Volmer–Heyrovsky–Tafel case) and $u = 0$ (thin lines) and $u = 20$ (thick lines). It should be taken into account that $u > 0$ for the HER [13,18]. A similar analysis was made for the Volmer–Tafel case shown in Figs. 3 and 4, which is illustrated in Fig. 9 (without the first cycle in Fig. 9b). It can be observed that both, the surface coverage and the relationship $j^{vol}(\eta, v_s)/j^{ss}(\eta)$, decrease when the parameter u increases.

Consequently, the most unfavorable condition for the relationship $j^{vol}(\eta, v_s)/j^{ss}(\eta)$ is obtained for $u = 0$ (Langmuir-type adsorption). This result is completely predictable, as the increase in the parameter u produces a decrease in the tran-

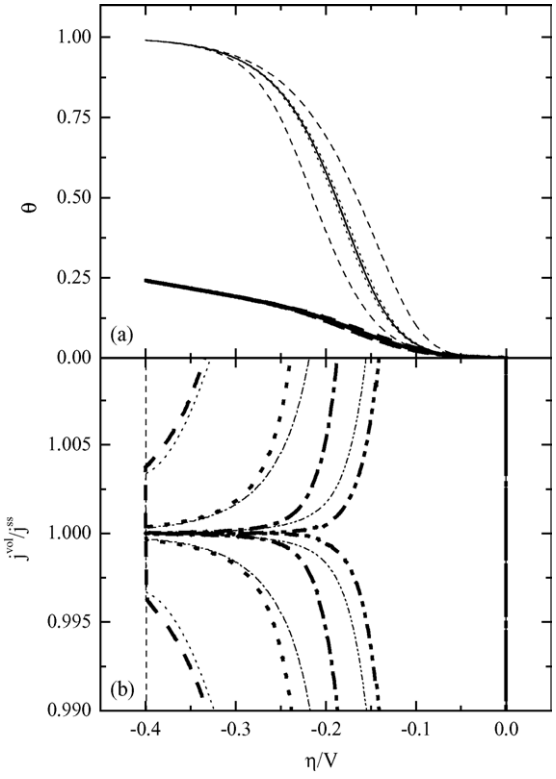

Fig. 9. Dependences (a) $\theta(\eta, v_s)$ and (b) $j^{vol}(\eta, v_s)/j^{ss}(\eta)$. $\theta^e = 10^{-3}$; $m_T = 10^{-5}$; $m_H = 0$; m_s (V cm^2 mol^{-1}): (–···–) 10^6, (-·-·-) 10^7, (···) 10^8, (- - -) 10^9 and (—) steady state. First cycle not included in (b). Thin lines: Langmuir-type adsorption. Thick lines: Frumkin-type adsorption, $\lambda = 0.5$, $u = 20$.

sient adsorption pseudocapacitance $C^t_\theta(\eta, v_s)$ [19,20], and therefore a larger range of overpotentials is needed in order to produce the same change in the surface coverage. This result can also be demonstrated from Eq. (9). Therefore, at any overpotential, the difference between the surface coverage corresponding to the voltammetric sweep response and that of the steady state condition is greater for Langmuir than for Frumkin adsorption. Consequently, the use of a Frumkin-type behavior for the adsorbed hydrogen does not describe the most unfavorable cases and besides makes the calculation more complex. Therefore, the Langmuir-type adsorption is appropriate for the description of the behavior of the adsorbed intermediate for the purpose of the present work.

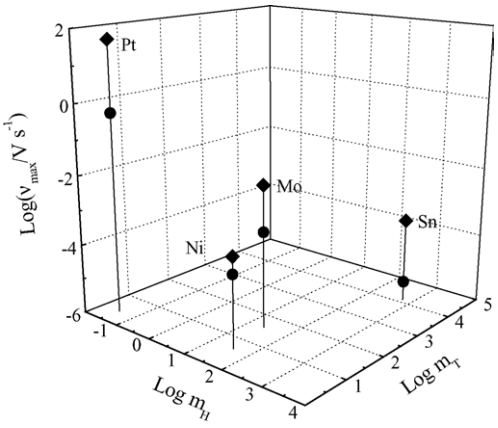

Fig. 10. Dependence of $\log(v_s^{max})$ on ($\log m_H$, $\log m_T$) for several metals fulfilling constrain given by (♦) Eq. (12) and (●) Eq. (17).

3.4. Applications

The equilibrium polarization resistance of the hydrogen electrode reaction can be evaluated directly from the experimental dependence $j^{exp}(\eta)$ near the equilibrium potential [10,11,15,16]. It can be also determined through Eq. (13), by the use of kinetic parameters calculated from experimental determinations run at high overpotentials [8,21–23]. Then, it is possible to replace these R_p values into Eq. (17) in order to find the maximum sweep rate that fulfills the relationship $j^{exp}(\eta, v_s) \cong j^{ss}(\eta)$.

Table 1 contains the values of the equilibrium polarization resistance on several metals, as well as the kinetic parameters when this information was available. The corresponding values of v_s^{max} were calculated for all cases by means of Eq. (17) and are indicated in the last column of Table 1. For those metals which kinetic parameters were known, v_s^{max} was also evaluated through the system of Eqs. (1), (7a)–(7c) and (9)–(11) and the constrain given by Eq. (12) and the corresponding values are also included in Table 1. Fig. 10 illustrates for these metals both values of v_s^{max}, that obtained from Eq. (17) and that calculated from the kinetic parameters. It can be appreciated that these last points are placed above, as it was expected. This means that if for these four metals the sweep rate is selected on the basis of the Eq. (17), the fulfillment of $j^{exp}(\eta, v_s) \cong j^{ss}(\eta)$ is guaranteed.

Table 1
Maximum scan rates calculated from kinetic parameters and/or R_p for several metal electrodes

Electrode	Electrolyte	T (°C)	m_H	m_T	R_p (Ω cm^2)	v_s^{max} (V s^{-1}) from Eq. (12)	v_s^{max} (V s^{-1}) from Eq. (17)
Pt [15]	H_2SO_4, 0.5 M	30	0.03278	2.6296	0.546	52.1	6.04×10^{-1}
Ir [16]	H_2SO_4, 2N	29			18.87		1.75×10^{-2}
Rh [16]	H_2SO_4, 2N	29			25.00		1.32×10^{-2}
Au [21]	H_2SO_4, 1.3N	25			29.70		1.11×10^{-2}
Mo [8,22]	HCl, 0.1N	25	24.272	37.581	531[a]	1.13×10^{-2}	6.21×10^{-4}
Ni [8]	NaOH, 2M	30	37.024	4.510	2544[a]	3.58×10^{-4}	1.30×10^{-4}
Sn [8,23]	Synthetic seawater	22	583.6	13567	83916[a]	2.72×10^{-4}	3.93×10^{-6}

[a] Calculated from v_i^e data.

4. Conclusions

The determination of the kinetic parameters of the hydrogen evolution reaction corresponding to the Volmer–Heyrovsky–Tafel mechanism through the use of the voltammetric response $j^{vol}(\eta)$ of a potentiodynamic sweep at a scan rate v_s has been analyzed. The system of equations for the evaluation of the dependences $\theta(\eta, v_s)$ and $j^{vol}(\eta, v_s)$ has been derived and simulated from numerical analysis for a wide range of kinetic parameters. On the basis of the results obtained, the conditions under which the dependence $j^{vol}(\eta, v_s)$ can be approximated to the steady state response $j^{ss}(\eta)$ have been developed and discussed. It has been also established a simple relationship between the maximum admissible scan rate v_s^{max} and the equilibrium polarization resistance R_p.

Acknowledgements

The financial support of Consejo Nacional de Investigaciones Científicas y Técnicas (CONICET), Agencia Nacional de Promoción Científica y Tecnológica (ANPCYT) and Universidad Nacional del Litoral (UNL) is gratefully acknowledged.

References

[1] M.R. Gennero de Chialvo, A.C. Chialvo, J. Electroanal. Chem. 415 (1996) 97.
[2] M. Okido, J.K. Depo, G.A. Capuano, J. Electrochem. Soc. 140 (1993) 127.
[3] A. Julic, J. Piljac, M. Metikos-Hokovic, J. Mol. Catal. A: Chem. 166 (2001) 293.
[4] L.M. Doubova, S. Trasatti, J. Electroanal. Chem. 467 (1999) 164.
[5] J. Perez, E. Gonzalez, H.M. Villullas, J. Phys. Chem. B 102 (1999) 10931.
[6] M.R. Gennero de Chialvo, A.C. Chialvo, Phys. Chem. Chem. Phys. 3 (2001) 3180.
[7] C.A. Marozzi, A.C. Chialvo, Electrochim. Acta 46 (2001) 861.
[8] M.R. Gennero de Chialvo, A.C. Chialvo, J. Electroanal. Chem. 448 (1998) 87.
[9] D.A. Harrington, B.E. Conway, Electrochim. Acta 32 (1987) 1703.
[10] B.E. Conway, L. Bai, J. Electroanal. Chem. 198 (1986) 149.
[11] P.M. Quaino, M.R. Gennero de Chialvo, A.C. Chialvo, Phys. Chem. Chem. Phys. 6 (2004) 4450.
[12] J.L. Fernández, M.R. Gennero de Chialvo, A.C. Chialvo, Phys. Chem. Chem. Phys. 5 (2003) 2875.
[13] J.H. Chun, K.H. Ra, N.Y. Kim, J. Electrochem. Soc. 149 (2002) E325.
[14] N. Krstajic, M. Popovic, B. Grgur, M. Vojnovic, D. Sga, J. Electroanal. Chem. 512 (2001) 16.
[15] J.P. Hoare, S. Schuldiner, J. Chem. Phys. 25 (1956) 786.
[16] T. Sasaki, A. Matsuda, J. Rest. Inst. Catal. Hokkaido Univ. 21 (1973) 157.
[17] M.R. Gennero de Chialvo, A.C. Chialvo, Electrochim. Acta 44 (1998) 841.
[18] F.M. Al-Faqeer, H.W. Pickering, J. Electrochem. Soc. 148 (2001) E248.
[19] J.M. Hale, R. Greef, Electrochim. Acta 12 (1967) 1409.
[20] B.E. Conway, E. Gileadi, Trans. Faraday Soc. 58 (1962) 2493.
[21] N. Pentland, J.O'M. Bockris, E. Sheldon, J. Electrochem. Soc. 104 (1957) 182.
[22] M.R. Gennero de Chialvo, A.C. Chialvo, Int. J. Hydrogen Energy 27 (2002) 871.
[23] R.P. Frankenthal, P.C. Milner, Corrosion 42 (1986) 51.